High Friction from a Stiff Polymer Using Microfiber Arrays

C. Majidi,[1,*] R. E. Groff,[1] Y. Maeno,[2] B. Schubert,[1] S. Baek,[1] B. Bush,[3] R. Maboudian,[3] N. Gravish,[4] M. Wilkinson,[4] K. Autumn,[4] and R. S. Fearing[1]

[1]*Department of Electrical Engineering & Computer Science, University of California, Berkeley, California 94720, USA*
[2]*Adhesive Tape Research Department, Nitto Denko Corporation, Umeda, Osaka 530-0001 Japan*
[3]*Department of Chemical Engineering, University of California, Berkeley, California 94720, USA*
[4]*Department of Biology, Lewis & Clark College, Portland, Oregon 97219, USA*

(Received 15 May 2006; published 18 August 2006)

High dry friction requires intimate contact between two surfaces and is generally obtained using soft materials with an elastic modulus less than 10 MPa. We demonstrate that high-friction properties similar to rubberlike materials can also be obtained using microfiber arrays constructed from a stiff thermoplastic (polypropylene, 1 GPa). The fiber arrays have a smaller true area of contact than a rubberlike material, but polypropylene's higher interfacial shear strength provides an effective friction coefficient of greater than 5 at normal loads of 8 kPa. At the pressures tested, the fiber arrays showed more than an order of magnitude increase in shear resistance compared to the bulk material. Unlike softer materials, vertical fiber arrays of stiff polymer demonstrate no measurable adhesion on smooth surfaces due to high tensile stiffness.

DOI: 10.1103/PhysRevLett.97.076103 PACS numbers: 46.55.+d, 62.25.+g, 68.35.−p, 81.40.Pq

High-friction, low-adhesion materials are important for applications such as automobile tires and shoes. Since surface roughness limits contact area, soft materials have typically been used to obtain high friction [1]. Dry friction of stiff polymers ($E \approx 1$ GPa) [2,3] and rubbers [1,4,5] on glass is a well studied area, with rubber friction coefficients an order of magnitude or more greater than stiff polymer. Alternatively, stiff materials in ordered fiber arrays [6,7] can have an effectively high compliance, permitting high contact area on rough surfaces. By appropriate choice of fiber array geometry, frictional and adhesion properties can be controlled.

Let the coefficients μ and $\hat{\mu}$ denote the ratio of shear resistance to applied load for smooth surfaces and fiber arrays, respectively. Recent work with vertically aligned multiwalled-carbon-nanotubes (VACNT) has shown friction coefficients of $\hat{\mu} = 0.795$ on glass (a 9× increase over free nanotubes) with 50 μm long fibers [8] and $\hat{\mu} = 2.2$ on a 20 μm radius gold sphere [9]. For long fibers and high enough surface energy [10], VACNT can make side contact under high preloads (20 N/cm^2) and show both tensile (11.7 N/cm^2) and shear adhesion (7.8 N/cm^2) [11]. Normal adhesion of VACNT samples is particularly pronounced at the nanoscale, where tests performed with a scanning probe microscope indicate a pull-off strength of 20 nN over an area of 0.001 μm^2 [12]. In this Letter, we show that a relatively stiff thermoplastic fiber array can provide high shear resistance without adhesion over a macroscopic area of 1.27 cm^2. Shear resistance in a polypropylene fiber array is increased by more than a factor of 10 compared to flat polypropylene film.

Fiber arrays were synthesized by casting one layer of 25.4 μm thick polypropylene film (TF-225-4, Premier Lab Supply Inc.) into a 20 μm thick polycarbonate filter (ISOPORE, Millipore Inc.) of 0.3, 0.6, or 2.5 μm pore radius. The polycarbonate filter was pressure filled in a vacuum oven for 25 minutes at 200 °C and then dissolved in methylene chloride. The array of fibers (Fig. 1) show height variation and only a slight amount of clumping [13] due to a relatively low surface energy compared with other polymers.

Static friction measurements were performed on a traditional pulley apparatus, where the sample was loaded in shear by a string run over a pulley to a hanging weight. The polypropylene sample was placed on an acetone-cleaned glass slide and subject to a constant normal load by a brass weight on a rigid flat platform. The shear load was increased until first sliding was observed. Experiments were performed on arrays of 0.3, 0.6, and 2.5 μm radius polypropylene fibers as well as two types of controls. One control was the unprocessed 25.4 μm thick polypropylene film and the other was processed film that underwent the same fabrication steps as the fiber arrays with the exception

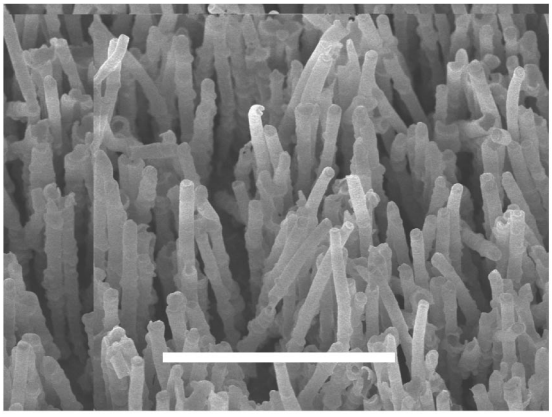

FIG. 1. SEM of an array of 20 μm long, 0.6 μm diameter polypropylene fibers etched from a polycarbonate membrane; scale bar represents 10 μm.

that no polycarbonate mold was included in the vacuum bake.

As shown in Fig. 2, high friction was observed in arrays of 0.3 μm radius polypropylene fibers over pressures of 0.17 to 0.79 N/cm^2. Under 0.79 N/cm^2 normal stress, the 0.3 μm radius polypropylene fiber arrays had an average friction coefficient $\hat{\mu} = 5.3$ (sample size = 15). The friction coefficient $\mu = 0.3$ for the processed control is similar to that measured in other experiments of polypropylene on smooth glass [2,3].

The experimental results suggest that altering the surface geometry of polypropylene can increase the coefficient of friction by an order of magnitude. This phenomenon is consistent with an adhesion theory of friction, in which shear resistance V has an affine relationship with the real area of contact A_r [14]. Because of the high elastic modulus of polypropylene ($E = 1$ GPa), the real area of contact for a nominally smooth control will be negligible. A fiber array, however, will exhibit high compliance due to fiber buckling and bending, thus enabling substantial interfacial contact even under low normal loads.

The adhesion theory may also explain why, under high pressure, shear resistance is greatest with the $R = 0.6$ μm arrays. This is evident in Fig. 2 for a compression of 16.5 N/cm^2. Based on image processing of the polycarbonate filters, these arrays were found to have a higher area fraction (25%) than the $R = 0.3$ μm (12%) or $R = 2.5$ μm (6%) arrays. That is, for higher loads when all fibers are in contact, the $R = 0.6$ μm arrays achieve a larger contact area and thus exhibit a greater shear resistance.

For a micro-rough substrate and/or small variations in fiber length, only a fraction of the fibers will be in contact under a small total normal load F. Fiber compliance can be modeled using either an ideal elastic column with a critical buckling load [7] or an inclined cantilever [15]. The fiber compliance is highly dependent on the slip condition at the contact [16]. For nonslip contact, the fiber is constrained to deform in a clamped-pinned or clamped-clamped mode and will be several times more stiff than a fiber under clamped-free loading.

A comparison of the theoretical force response for the various deformation modes of an $R = 0.3$ μm fiber array is presented in Fig. 3. Here, a 5.17 cm radius probe is pressed into the array by a distance Δ. Noting that the radius of contact is small relative to the probe radius, the force response is approximately $2\pi p \rho F_{cr} \Delta$ for an array of ideal columns, and $\pi p \rho k \Delta^2$ for inclined cantilevers, where p is the probe radius, $\rho = 42 \times 10^6$ cm^{-2} is the fiber density, F_{cr} is the critical buckling load, and k is the stiffness of an inclined cantilever. In general, $F_{cr} = K\pi^2 EI/L^2$ [17], where K is a geometric factor that depends on the buckling mode, $E = 1$ GPa is the elastic modulus, $I = \pi R^4/4$ is the area moment of inertia, and $L = 20$ μm is the fiber length. For clamped-free loading, in which the fiber tip can slide freely with respect to the contacting substrate, $K = 1/4$ and so $F_{cr} = 39$ nN. The stiffness of an inclined cantilever is approximately $k = 3EI/L^3 \sin^2\theta$ [15,16], where θ is the angle of natural deflection from vertical.

Also plotted in Fig. 3 is a typical force response obtained experimentally using an optical force sensor. Among the various column buckling models, the clamped-free mode

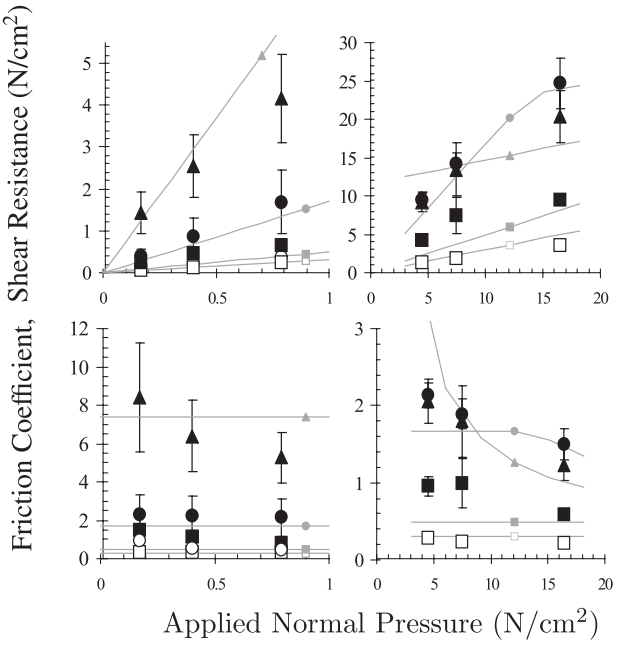

FIG. 2. Plot of normal pressure vs shear resistance for polypropylene fiber arrays and controls; (▲) radius $R = 0.3$ μm, (●) $R = 0.6$ μm, (■) $R = 2.5$ μm, (○) unprocessed control, (□) processed control; (left) loading area = 1.27 cm^2, sample size = 15; (right) loading area = 0.033 cm^2, sample size = 5; error bars represent 1 standard deviation in the data; solid lines represent theoretical predictions from Eqs. (1)–(3) for $R_t = 3R$.

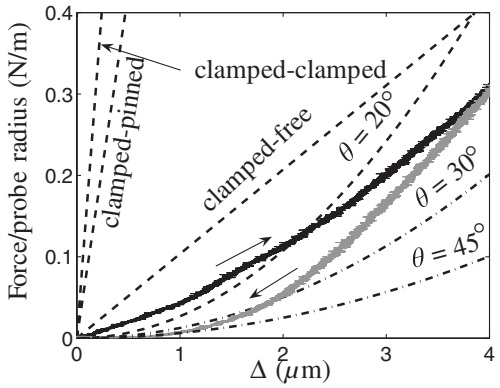

FIG. 3. Force response of $R = 0.3$ μm fiber array indented by a spherical probe (radius = 5.17 cm); greater compliance at low Δ may be a result of fiber sparsity near the top of the array due to length variation; (dashed line) theoretical predictions based on ideal column buckling for various buckling modes; (dash-dotted line) cantilever bending model for various angles of inclination from vertical; arrows indicate loading direction.

most closely matches the measured response. At lower indentations, however, it overestimates the stiffness. This may be a result of fiber length variation, which causes the array to be more sparse at heights close to 20 μm. Regardless, the clamped-free buckling model will be adopted for the remaining analysis, as it is the most tractable and produces a reasonable estimate of the mechanical response.

Under a light normal load F, it follows that for an array of ideal elastic columns, the number of contacts will be approximately $N = F/F_{\mathrm{cr}}$. With the addition of shear load, N should be slightly greater due to the enhanced compliance of columns under compound loading, but this difference is assumed to be negligible. By Coulomb's law, the shear resistance from each contact will be $V_f = \mu F_{\mathrm{cr}} + \tau A_f$, where $\tau \approx 10$ MPa [2,3] is the interfacial shear strength per unit area and A_f is the real area of contact for the fiber. Since the applied load F_{cr} is constant, A_f is also likely to be constant. The shear resistance of an entire array is $V = V_f N$, and so substituting the expressions for N and V_f, it follows that

$$V = \hat{\mu} F \quad \text{and} \quad \hat{\mu} = \mu + \tau A_f / F_{\mathrm{cr}}. \tag{1}$$

Interestingly, (1) resembles Amontons' law with $\hat{\mu}$ as an effective coefficient of friction.

The ideal column model also implies complete contact when the applied load exceeds $F_{\mathrm{cr}} N_0$, where N_0 is the total number of fibers inside the contact area. In this case,

$$\hat{\mu} = \mu + \tau N_0 A_f / F, \quad (F > F_{\mathrm{cr}} N_0) \tag{2}$$

and A_f can no longer be approximated as constant. Since $N_0 A_f$ is bounded above by the apparent area of contact, (2) implies that $\hat{\mu}$ should asymptotically approach μ with increasing load F. The reduction in $\hat{\mu}$ with increasing F is apparent in Fig. 2 and Table I.

Table I compares the response of various structures to two different compressive loads: 0.79 N/cm^2 over 1.27 cm^2 and 16.5 N/cm^2 over 0.033 cm^2. Based on the model, the real area of contact A_r is given by $A_r = F(\hat{\mu} - \mu)/\tau$. The fraction of fibers that are buckled (in contact) is evaluated as $f = N/N_0$, where $N = \min\{F/F_{\mathrm{cr}}, N_0\}$, and the average contact area per fiber is $A_f = A_r/N$. Under 0.79 N/cm^2 compression, only a minority of fibers are buckled in each of the three fiber arrays. The effective coefficient of friction $\hat{\mu}$ is highest when operating in this regime. With a higher compressive load of 16.5 N/cm^2, all fibers in the $R = 0.3$ μm and $R = 0.6$ μm arrays buckle under a force of approximately F/N_0. In this case, the load controlled friction, $\mu(F/N_0)$, is expected to overshadow the adhesion term τA_f, leading to the observed drop in $\hat{\mu}$.

The estimates for A_f are compared to Johnson-Kendall-Roberts theory [18], which predicts a contact area of

$$A_{\mathrm{JKR}} = \pi \left[\frac{3(1-\nu^2)R_t}{4E} \left(F_{\mathrm{cr}} + 3\pi W_{\mathrm{ad}} R_t + \sqrt{6\pi W_{\mathrm{ad}} F_{\mathrm{cr}} R_t + (3\pi W_{\mathrm{ad}} R_t)^2} \right) \right]^{2/3}, \tag{3}$$

where R_t is the radius of curvature, ν is Poisson's ratio, and W_{ad} is the interfacial work of adhesion. We let $\nu = 0.3$, a typical value for polypropylene [19], and $W_{\mathrm{ad}} = 75$ mJ/m^2 [20]. Table I presents values for A_{JKR} based on the assumption $R_t = 3R$, as this provides a reasonable fit to the data and approximates the blunted shape of the tips. When $f = 1$, F_{cr} is replaced by F/N_0 in evaluating (3). Theoretical predictions for $\hat{\mu}$ based on (1)–(3) for $R_t = 3R$ are plotted along with the experimental results in Fig. 2. It is important to note that observations under SEM clearly indicate that the fiber tips are not rounded and so JKR theory may not be applicable. It is also possible that some of the fibers may be engaged in side contact [10].

Measurements performed with a two-axis force sensor demonstrate that fiber arrays also exhibit high dynamic friction. The force sensor consists of four double cantilevers with optical displacement sensors. Each sample was glued to a nanopositioning stage (NanoCube, PI) and contacted by a spherical glass probe of radius 5.17 cm. A plot of shear force (V) and normal load (F) is presented in Fig. 4. The probe was pressed vertically into an $R = 0.3$ μm array, dragged across the array at a fixed height, and then retracted vertically. The normal load dropped as the array was sheared, since a fiber requires less normal load to remain bent to a specified height in the presence of shear. After an initial drag, a static coefficient of $\hat{\mu} = V/F \approx 2.8$ was recorded, while experiments on the controls exhibited static coefficients similar to those observed in the pulley experiments. Microscopic observation reveals

TABLE I. Estimated contact areas for polypropylene fiber arrays; ρ is the fiber density, f is the estimated fraction of fibers buckled in the clamped-free mode ($K = 1/4$).

Load (N/cm^2)	Radius (μm)	ρ (cm^{-2})	$\hat{\mu}$	A_r (mm^2)	A_f (μm^2)	A_{JKR} (μm^2)	f
0.79	0.3	42×10^6	5.3	0.5	0.02	0.028	0.48
	0.6	22×10^6	2.1	0.18	0.11	0.086	0.057
	2.5	0.42×10^6	0.81	0.05	9.7	3.6	0.001
16.5	0.3	42×10^6	1.2	0.049	0.035	0.028	1.0
	0.6	22×10^6	1.5	0.065	0.089	0.086	1.0
	2.5	0.42×10^6	0.58	0.015	5.3	3.6	0.20

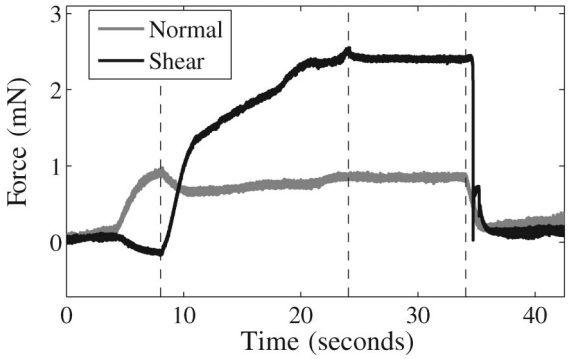

FIG. 4. Applied normal load and shear resistance vs time for an array of 0.3 μm radius polypropylene fibers. Dotted lines from left to right indicate (i) transition from vertical approach to horizontal drag at 5 μm/s, (ii) pause after drag, and (iii) vertical retraction.

that gluing the sample to a rigid surface introduces roughness on the order of the fiber length, which may be why the value for $\hat{\mu}$ measured with the two-axis sensor is significantly less than that with the pulley apparatus.

It is important to note in Fig. 4 that the normal load appears positive over the entire loading cycle, indicating that the array supports only compression and does not produce any tensile resistance during normal pull off. That is, although the sample exhibits enhanced friction, it has negligible adhesion—a rare property among high-friction materials contacting smooth surfaces. Unlike intrinsically compliant materials, an array of vertical columns exhibits enhanced compliance only in the compressive direction—fiber length variations and elastic restoring forces will lead to vanishing A_r under zero or tensile loading. To obtain compliance in the tensile direction, curved fibers [23] or compound cantilever fibers [24] can be used. By selecting the appropriate aspect ratio, such structures can satisfy the Dahlquist criterion [25] in both compression and tension, suggesting the possibility of dry adhesion. However, as discussed in [16], friction between the fiber tip and substrate can significantly reduce the compliance and so additional modifications to the fiber or backing geometry may be required.

In summary, a microcasting process has been shown to transform a low friction material ($\mu = 0.3$) into a high-friction structure with a coefficient of $\hat{\mu} = 5.3$ under 0.79 Ncm^2 of pressure. Such frictional behavior approaches rubber [$\tau = 0.25$ MPa [5]], which, under the same pressure, is expected to have a coefficient of $\mu = 0.25/0.0079 = 32$. This behavior is achieved by molding polypropylene into an array of microfibers, resulting in a compliant structure that allows significant interfacial contact even under light pressure. Friction enhancement through increased compliance is consistent with an adhesion theory of friction. A quantitative prediction for the enhanced coefficient of friction $\hat{\mu}$ is obtained by treating the fibers as ideal elastic columns subject to Coulomb's friction law.

This work was supported by a IC (R. E. G.), DARPA, NSF NIRT (No. EEC-034730), NSF NSEC, and Emhart Corporation.

*Electronic address: cmajidi@eecs.berkeley.edu

[1] B. N. J. Persson, O. Albohr, U. Tartaglino, A. Volokitin, and E. Tosatti, J. Phys. Condens. Matter **17**, R1 (2005).
[2] C. M. Pooley and D. Tabor, Proc. R. Soc. A **329**, 251 (1972).
[3] D. H. Gracias and G. A. Somorjai, Macromolecules **31**, 1269 (1998).
[4] A. Roberts and S. Jackson, Nature (London) **257**, 118 (1975).
[5] M. Barquins and A. Roberts, J. Phys. D **19**, 547 (1986).
[6] D. Campolo, S. Jones, and R. S. Fearing, *Proceedings from the Third IEEE Conference on Nanotechnology, San Francisco, CA, 2003* (IEEE, New York, 2003), Vol. 2, pp. 856–859.
[7] A. Jagota and S. J. Bennison, Integr. Comp. Biol. **42**, 1140 (2002).
[8] P. Dickrell, S. Simon, D. Hahn, N. Raravikar, L. Schadler, P. Ajayan, and W. Sawyer, Tribol. Lett. **18**, 59 (2005).
[9] H. Kinoshita, I. Kumme, M. Tagawa, and N. Ohmae, Appl. Phys. Lett. **85**, 2780 (2004).
[10] C. Majidi, R. E. Groff, and R. S. Fearing, J. Appl. Phys. **98**, 103521 (2005).
[11] Y. Zhao, T. Tong, L. Delzet, A. Kashani, M. Meyyappan, and A. Majumdar, J. Vac. Sci. Technol. B **24**, 331 (2006).
[12] B. Yurdumakan, N. R. Raravikar, P. M. Ajayan, and A. D. Dhinojwala, Chem. Commun. (Cambridge) **2005**, 3799 (2005).
[13] C. Majidi, R. Groff, and R. Fearing, *Proceedings of the IMECE* (ASME, New York, 2004).
[14] E. Rabinowicz, *Friction and Wear of Materials* (Wiley, New York, 1995), 2nd ed., Chap. 4.
[15] M. Sitti and R. S. Fearing, J. Adhes. Sci. Technol. **17**, 1055 (2003).
[16] K. Autumn, C. Majidi, R. Groff, A. Dittmore, and R. Fearing, J. Exp. Biol. (to be published).
[17] J. M. Gere and S. P. Timoshenko, *Mechanics of Materials* (PWS-Kent, Boston, MA, 1984).
[18] K. L. Johnson, K. Kendall, and J. Roberts, Proc. R. Soc. A **324**, 301 (1971).
[19] MatWeb, http://www.matweb.com, 2006.
[20] The water contact angles measured on our processed (85°) and unprocessed (95°) control samples were consistent with values obtained by [3] and so we adopt their measured surface energy for polypropylene: $\gamma_1 \approx 30$ mJ/m^2 [2,3]. The surface energy of glass is $\gamma_2 \approx 47$ mJ/m^2 [21] and so, assuming that dispersive forces dominate, $W_{ad} \approx 2\sqrt{\gamma_1 \gamma_2} = 75$ mJ/m^2 [22].
[21] Accudyne, http://www.accudynetest.com, 2006.
[22] J. Israelachvili, *Intermolecular and Surface Forces* (Academic, New York, 1992).
[23] B. N. J. Persson, J. Chem. Phys. **118**, 7614 (2003).
[24] R. Fearing and M. Sitti, U.S. Patent No. 6 872 439 2005.
[25] A. V. Pocius, *Adhesion and Adhesives Technology* (Carl Hanser Verlag, Munich, Germany, 2002).